Available online at www.sciencedirect.com
ScienceDirect
Applied Surface Science 253 (2007) 9430–9434
applied surface science
www.elsevier.com/locate/apsusc

Preparation of hybrid film with superhydrophobic surfaces based on irregularly structure by emulsion polymerization

Ailan Qu *, Xiufang Wen, Pihui Pi, Jiang Cheng, Zhuoru Yang

The School of Chemical and Energy Engineering, South China University of Technology, Guangzhou 510640, China

Received 2 April 2007; received in revised form 4 June 2007; accepted 4 June 2007
Available online 9 June 2007

Abstract

A superhydrophobic surface originated from quincunx-shape composite particles was obtained by utilizing the encapsulation and graft of silica particles to control the surface chemistry and morphology of the hybrid film. The composite particles make the surface of film form a composite interface with irregular binary structure to trap air between the substrate surface and the liquid droplets which plays an essential role in obtaining high water contact angle and low water contact angle hysteresis. The water contact angle on the hybrid film is determined to be $154 \pm 2^\circ$ and the contact angle hysteresis is less than 5°. This is expected to be a simple and practical method for preparing self-cleaning hydrophobic surfaces on large area.

Keywords: Hybrid fluoropolymer; Superhydrophobic surface; Hierarchical irregularly structure; Silica particles

1. Introduction

Superhydrophobic surfaces are currently a subject of great interest and enthusiastic study because of their various important applications. In general, the water contact angles (WCA) on smooth hydrophobic surfaces are not exceeding 120°, even when coated with a monolayer of perfectly close-hexagonal-packed-CF_3 groups [1]. On some natural tissues, however, such as lotus leaves or Lepidoptera wings, the WCA can reach as high as 160° or above, and a water droplet can freely roll off on these surfaces without leaving any trace of beads [2]. Lotus leaf is covered by many papillae with a diameter in the range of 3–10 μm, while these papillae are decorated with smaller protrusions of nanometer size. Such special micro-nano-binary structure increases the surface roughness dramatically, making air trapped in the grooves underneath the liquid and minimizes the contact area between the leaf and the liquid [3,4]. Recently, hierarchical regularly or irregularly structured surfaces, exhibiting roughness on various length scales, have gained increasing interest because they might theoretically make any substrates superhydrophobic in despite of their surface chemistry [5,6]. The demands to design and fabricate the surfaces with appropriate roughness characteristics also motivate people to explore the physical and chemical mechanisms of material properties at the micro- or nanoscale. Up to now, many superhydrophobic surfaces have been fabricated by these approaches including etching and lithography [7–12], addition of a sublimation material [6,13], chemical vapour deposition [14–17], phase separation [18–22], sol–gel processing [23–26], and self-assembly [27–31]. Nevertheless, most of these reported approaches are restricted in rigorous experimental conditions and multi-step processes or complicated instruments. This means that they cannot be easily scaled-up to practical systems. Such coatings with formation of appropriate surface patterns on hydrophobic surfaces are of great technical interest, especially if aqueous media are concerned. For this reason, various fluorine containing nanocomposite coatings have been developed by sol–gel processing. The morphology of these hydrophobic surfaces has been controlled by varying the content of silica particles regarding size, degree of aggregation, and concentration. In this paper, we adopted a practical procedure for preparing a superhydrophobic aqueous coating with irregular surface structure by using silica particles.

* Corresponding author. Tel.: +86 13710228756; fax: +86 20 87112057 804.
E-mail address: qal67@163.com (A. Qu).

0169-4332/$ – see front matter © 2007 Elsevier B.V. All rights reserved.
doi:10.1016/j.apsusc.2007.06.002

2. Experimental

Silicon dioxide particles were prepared according to well-known Stöber method [32] which is very convenient to manipulate the particle size. A 500 mL absolute ethanol, 35 mL aqueous solution of ammonia were introduced in a 1000-mL, three-neck, round-bottom flask equipped with a heat exchange system. The mixture was stirred at 300 rpm to homogenize and heated at 50 °C. After stabilization, 15 mL of tetraethoxysilane (TEOS) was added quickly and reaction occurred at the chosen temperature with constant stirring for 24 h. To graft polymerizable groups onto the silica surface, the silica particles were modified with methacryloxypropyl trimethoxysilane (MATMS, at a dosage of 0.3 g per gram silica particles by assuming 100% conversion of TEOS). After the mixture was stirred for 10 h at ambient temperature, the reaction medium was heated to 80 °C for 2 h to promote covalent bonding of the organosilane to the surface of the silica nanoparticles. When the synthesis of silica particles was completed, the main part of ethanol and ammonia was evaporated under reduced pressure and was replaced with water. The final concentration of silica suspensions was determined by measuring the mass.

Emulsion polymerization was performed in the presence of modified silica particles (50% mass ratio of monomers). Following a typical recipe, the given amount of dealt silica suspension (a mixture of water/ethanol = 80/5 with a part of surfactants) was transferred into a thermostated reactor with continuous stirring. A nonylphenol poly(oxyethylenic) non-ionic surfactant (OP-10) and a reactive anionic surfactant (DNS-86, allyloxy polyoxyethylene(10)nonyl ammonium sulfate) were used as emulsifier at 0.8% (OP/DNS-86 = 5/3 wt) of total solution. After the mixture was stirred for 1 h, the pre-emulsified (20 wt% based on total monomers) methyl methacrylate (MMA, 97%) and a part of potassium persulfate (KPS) (1.0% wt in total) were added dropwise. Then a pre-emulsified mixture of MMA, butyl acrylate (BA, 96%), 2-hydroxyethyl methacrylate (HEMA, 98%) and α-methyl acrylic acid (MAA, 98%) as first shell, and the pre-emulsified mixture of 40–60 wt% dodecafluoroheptyl methacrylate (DFMA) and 6 wt% γ-methacryloxypropyltriisopropoxidesilane (MAPTIPS) as second shell were added subsequently. The polymerization started at 75 °C and finished within 6 h. After the reaction was kept for 2 h, the other part of modified silica (50 wt%) suspension was introduced into the reactor, and MAPTIPS (5 wt%) was added at the same time. The total amount of monomers is 200 g/L and the ratio between different kinds of monomers may be adjusted according to glass transition temperature. The film of composite latex was prepared by coating on glass slides to be dried at room temperature for 2 days and nights.

The morphologies of singular diameter and composite particles were obtained by transmission electron microscopy (TEM, Tecnai 10, Philips Corporation, Holand). The samples were observed directly without further staining for improving contrast. Atomic force microscopy (AFM) measurement was performed using a Dimension 62000 nm instrument (CSPM2000). Images were acquired under ambient conditions in tapping mode using a Nanoprobe cantilever. Contact angle for water (WCA) was measured with an OCA15 contact angle goniometer from Dataphysics Co. Germany. Typically, the average value of five measurements, made at different positions of the film surface was adopted as the value of WCA. X-ray photoelectron spectroscopy (XPS) data were collected in both survey and high-resolution mode on Krafos Axis Ultra DCD systems equipped with a Al Kα source and operating at 150 W. Scanning scope is 700 μm × 300 μm. Data were recorded at 30°, 60° and 90° takeoff angles, respectively. These angles correspond to the approximate sampling depth of 20–100 Å. Semiquantification was done by integration of the atomic signals and corrected with sensitivity factors adjusted for the instrument lens and detector design.

3. Result and discussion

As shown in Scheme 1, the composite particles with quincunx-shaped irregular structure were prepared. The morphology of hybrid latex particles was observed by TEM as shown in Fig. 1. The samples were observed directly without

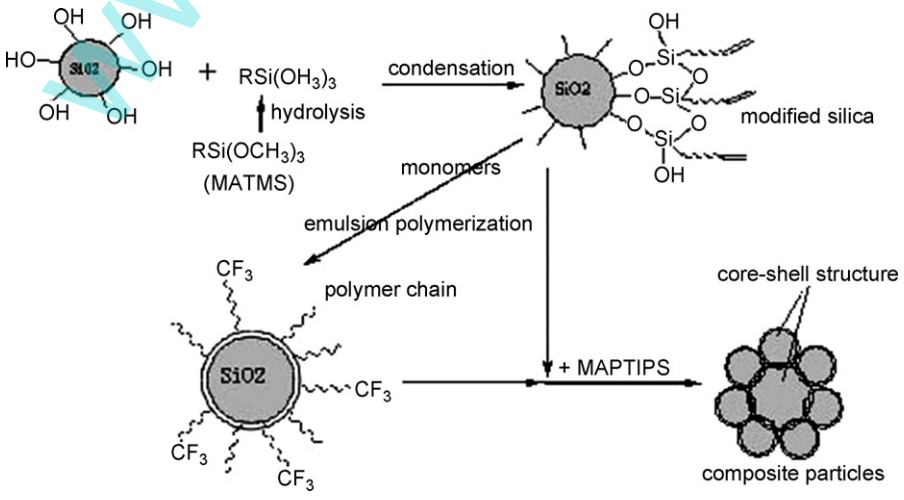

Scheme 1. The procedure for preparing composite latex particles.

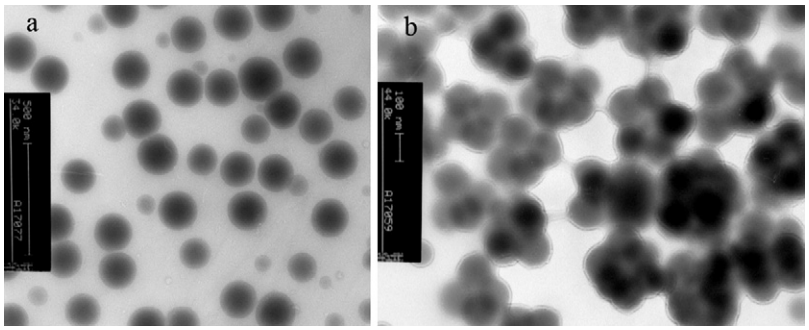

Fig. 1. TEM images of composite latex particles (a and b: before and after adding the second part of silica particles, respectively).

staining. In Fig. 1a, it can be seen that the hybrid latex particles before the addition of second part of silica showed clearly core-shell structure based on silica core (in dark) and polymer shell (in light). When the second part of silica particles was introduced, the shape of composite particles became quincunx-shape (Fig. 1b) due to the covalent bonding of the organosilane to the silica surface and the copolymerization between silica and latex particles resulted from the MAPTIPS.

The wettability of the composite film is evaluated using a contact angle goniometer shown in Fig. 3. The water contact angle hysteresis (WCAH, the difference between advancing and receding contact angle) was determined by measuring advancing and receding water contact angles. It is surprised that the WCA is only $141 \pm 2^\circ$ and the water droplet is sticky on it even up to 90° tilt angle when the film was dried at room temperature for 12 h. However, after the film was kept in the air at room temperature for 2 months, the static water contact angle increased as high as $154 \pm 2^\circ$ while WCAH decreased to $3 \pm 1^\circ$. The water droplet is easy to slide when the glass was tiltled up to 32° and dust on the surface was cleaned. It may be attributed to the orientation on the surface of fluorine and silicon. The functional monomer MAPTIPS plays an important role in this process by decreasing surface energy of the film due to its effects of promotion and cooperation on fluorine surface self-assembling and serving as an anchor to the silica and substrate by forming covalent bonds. The effects of MAPTIPS and silica particles on gradient distribution of fluorine were discussed elsewhere.

To confirm the existence of fluorine containing groups on the layer of the prepared film, XPS spectrum was obtained on an axis ultramulti-technique electron spectrometer with an Al $K\alpha$ X-ray source and operating at 150 W. The F_{1s} window shows a singular symmetrical peak at 689.1 ± 0.1 eV, and the O_{1s} window shows two peaks with similar areas at 533.8 ± 0.1 eV and 532.3 ± 0.1 eV, respectively, corresponding to the two different types of oxygen in the ester functional group. There is also a peak of Si_{2p} which corresponds to Si–O at 102.1 eV. The C_{1s} window shows a complex pattern of peaks which stand for four kinds of carbon bonds (289.3 eV maybe attributed to C–F or C=O, the peak overlap resulted from the binding energy of any CF groups (ca. 289.6 eV) to be indistinguishable from that of C=O (289.4 eV), CF_3 at 293.8 eV, C–O at 286.1 eV and C–C at 285.0 eV). A typical C_{1s} spectrum for the film surface is given in Fig. 2.

At the same time, the changes of the orientation of fluorine and silicon on the film surface during drying at room temperature were analyzed by XPS spectrum, and the elements on different layers of the film surface were given in Table 1. Analysis performed at various take-off angles of 30, 60 and 90° provided a means to probe both the surface and deeper features of this material. As can be seen from Table 1, the fluorine content on surface is higher than that in the bulk (fluorine theoretic content is 20.35%, assuming 100% conversion of emulsion polymerization) and it decreases along with depth into the film. This indicated, as anticipated, that the

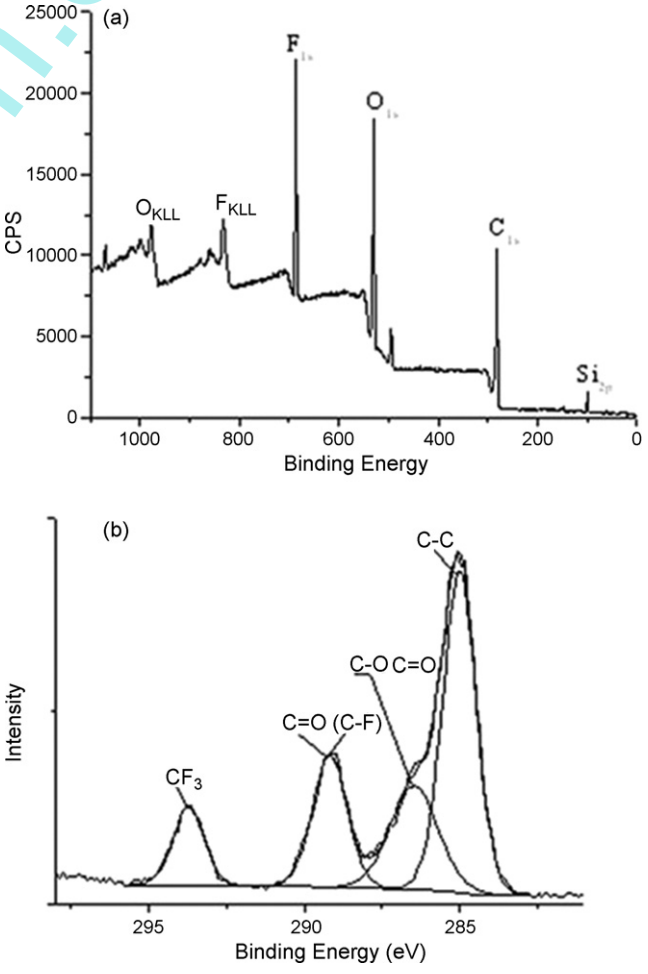

Fig. 2. XPS spectrum of hybrid film (a: survey; b: C_{1s} spectrum).

Table 1
XPS data for different, time of film formation

Time[a]	Take-off angle(°)	Atom percentages			
		F	C	O	Si
6 h	30	27.6	52.3	17.7	2.4
	60	27.2	54.3	16.3	2.1
	90	24.9	56.0	16.0	3.0
48 h	30	29.5	48.0	19.5	3.0
	60	28.5	51.2	17.7	2.7
	90	20.1	59.0	17.9	3.0
240 h	30	30.4	45.0	20.9	3.8
	60	29.6	48.9	18.7	2.8
	90	22.6	57.1	17.2	3.2
2 months	30	30.8	43.3	21.6	4.3
	60	29.9	48.5	18.9	2.7
	90	24.8	55.1	16.9	3.2

[a] *Note*: The time of film formation did not contain vacuum time in analysis instrument.

fluorocarbon side chain enriched preferentially on the surface compared to the acrylate backbone and a gradient of fluorine exists from surface to the bulk of polymer film. An orientable ability of silicon was also showed clearly from the data of silicon in Table 1. At the same time, it was indicated that the contents of fluorine and silicon on the film surface both increased with increasing the time of film formation. The increased ratio of fluorine is slight in the end while that of silicon is high which probably resulted in the increase of water contact angle and decrease of slide angle [33].

However, the result of WCA revealed that the wettability of the surface is not only governed by the surface energy of the materials but also by the surface roughness and structure. The surface roughness can change the contact angles as the chemicals do but through a different mechanism. Two distinct models have been proposed to explain this phenomenon: the Wenzel model and the Cassie model [22]. The Wenzel model describes a roughness regime in which both advancing WCA and WCA hysteresis (WCAH) increase as r increases (water penetrates into the surface cavity). The Cassie model describes that, as r further increases passing a critical level, the water receding angle also increases dramatically (water does not penetrate into the surface cavity; there is an air pocket between the water droplet and the solid surface), thus minimizing the WCAH [34]. The surface morphology of the film was observed using AFM as shown in Fig. 3, The results of preliminary quantitative analysis, such as root-mean-square roughness (Rms, which gives the standard deviation of the height values), surface roughness factor (R, $R = 1 + \mathrm{Sdr}$, Sdr is surface area ratio, which is the ratio between the interfacial and projected areas) and mean roughness (Ra), were obtained from AFM software analyses. The roughness factor is 2.16, the average surface roughness was estimated to be 32 nm over a scope of 20 μm × 20 μm.

The apparent water contact angle calculated from the Wenzel's model (121.5°, based on the 104° WCA of a flat fluorinated surface) is much lower than experimental value obtained (154°) in this work. This indicated that a composite

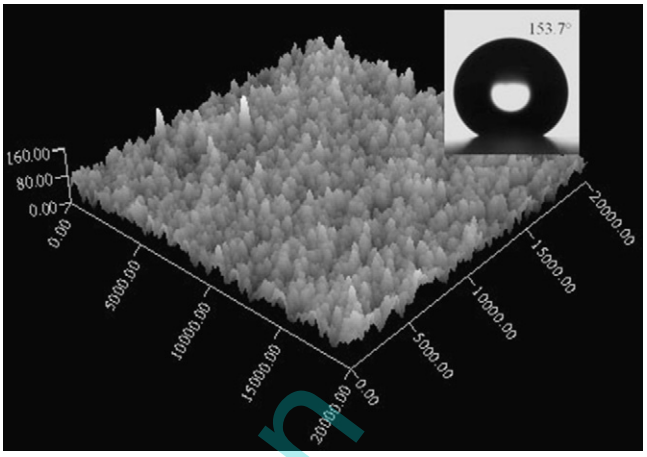

Fig. 3. AFM images of the hybrid film surface and WCA on it.

surface may be formed to allow air pockets to exist between the water droplet and the solid surface. For a composite surface, water contact angle is described by the Cassie–Baxter equation as follows:

$$\cos\theta_r^c = f\cos\theta + f - 1 \quad (1)$$

where f is the area fraction of the solid in contact with the liquid. The value of f was calculated to be 0.136. This result implies that water did not penetrate the surface grooves on the films.

On the other hand, this hybrid fluorinated emulsion has a good compatibility with modified silica particles for controlling the surface roughness easily. On the contrary, it is easy to aggregate when silica particles were combined with the pure fluorinated emulsion.

4. Conclusion

The self-clean hydrophobic coating with irregular structural composite particles has been synthesized by using emulsion encapsulation and graft process. These composite coating can be applied to various common substrates by using simple spray-coating or spin-coating methods to create super-hydrophobic surfaces with a water contact angle larger than 150°. Compared with other complex processes, this surface coating method is simpler and more feasible for practical self-cleaning applications.

Acknowledgment

We are grateful for the financial support from National Natural Science Foundation of China (Grant No. 20506005).

References

[1] G. Zhang, D. Wang, Z.Z. Gu, H. Möhwald, Langmuir 21 (2005) 9143.
[2] W. Barthlott, C. Neinhuis, Planta 202 (1997) 1.
[3] C. Neinhuis, W. Barthlott, Ann. Bot. 79 (1997) 667.
[4] L. Feng, S. Li, Y. Li, H. Li, L. Zhang, J. Zhai, Y. Song, B. Liu, L. Jiang, D. Zhu, Adv. Mater. 14 (2002) 1857.

[5] S. Herminghaus, Europhys. Lett. 52 (2000) 165.
[6] M. Miwa, A. Nakajima, A. Fujishima, K. Hashimoto, T. Watenabe, Langmuir 16 (2000) 5754.
[7] K. Teshima, H. Sugimura, Y. Inoue, O. Takai, A. Takano, Appl. Surf. Sci. 244 (2005) 619.
[8] B.T. Qian, Z. Shen, Langmuir 21 (2005) 9007.
[9] R. Furstner, W. Barthlott, C. Neinhuis, P. Walzel, Langmuir 21 (2005) 956.
[10] M. Callies, Y. Chen, F. Marty, A. Pepin, D. Quéré, Microelectron. Eng. 78–79 (2005) 100.
[11] M.E. Abdelsalam, P.N. Bartlett, T. Kelf, J. Baumberg, Langmuir 21 (2005) 1753.
[12] H. Notsu, W. Kubo, I. Shitanda, T. Tatsuma, J. Mater. Chem. 15 (2005) 1523.
[13] A. Nakajima, K. Hashimoto, T. Watanabe, K. Takai, G. Yamauchi, A. Fujishima, Langmuir 16 (2000) 7044.
[14] H. Liu, L. Feng, J. Zhai, L. Jiang, D.B. Zhu, Langmuir 20 (2004) 5659.
[15] L.B. Zhu, Y.H. Xiu, J.W. Xu, P.A. Tamirisa, D.W. Hess, C.P. Wong, Langmuir 21 (2005) 11208.
[16] L. Huang, S.P. Lau, H.Y. Yang, E.S.P. Leong, S.F. Yu, S. Prawer, J. Phys. Chem. B 109 (2005) 7746.
[17] A. Hozumi, O. Takai, Thin Solid Films 334 (1998) 54.
[18] A. Nakajima, K. Abe, K. Hashimoto, T. Watanabe, Thin Solid Films 376 (2000) 140.
[19] S. Minko, M. Muller, M. Motornov, M. Nitschke, K. Grundke, M. Stamm, J. Am. Chem. Soc. 125 (2003) 3896.
[20] H. Yabu, M. Takebayashi, M. Tanake, M. Shimomura, Langmuir 21 (2005) 3235.
[21] N.J. Shirtcliffe, G. McHale, M.I. Newton, C.C. Perry, Langmuir 19 (2003) 5626.
[22] H.Y. Erbil, A.L. Demirel, Y. Avci, O. Mert, Science 299 (2003) 1377.
[23] M. Hikita, K. Tanaka, T. Nakamura, T. Kajiyama, A. Takahara, Langmuir 21 (2005) 7299.
[24] H.M. Shang, Y. Wang, S.J. Limmer, T.P. Chou, K. Takahashi, G.Z. Cao, Thin Solid Films 472 (2005) 37.
[25] X. Wu, L. Zheng, D. Wu, Langmuir 21 (2005) 2665.
[26] W. Ming, D. Wu, R. van Benthem, G. de With, Nano Lett. 5 (2005) 2298.
[27] F. Shi, Z.Q. Wang, X. Zhang, Adv. Mater. 17 (2005) 1005.
[28] R.M. Jisr, H.H. Rmaile, J.B. Schlenoff, Angew. Chem. Int. Ed. 44 (2005) 782.
[29] J.T. Han, Y. Zheng, J.H. Cho, X. Xu, K. Cho, J. Phys. Chem. B 109 (2005) 20773.
[30] L. Zhai, F.C. Cebeci, R.E. Cohen, M.F. Rubner, Nano. Lett. 4 (2001) 1349.
[31] S. Pilotek, H.K. Schmidt, J. Sol-Gel Sci. Technol. 26 (2003) 789.
[32] W. Stöber, A. Fink, E. Bohn, J. Colloid Interface Sci. 26 (1968) 62.
[33] H. Murase, T. Fujibayashi, Prog. Org. Coat. 31 (1997) 97.
[34] C.M. Chan, G.Z. Cao, H. Fong, M. Sarikaya, J. Mater. Res. 15 (2000) 148.